

COORDINATED ANALYSIS OF AN EXPERIMENTALLY SPACE WEATHERED CARBONACEOUS CHONDRITE. M. S. Thompson¹, M. J. Loeffler², R. V. Morris³, S. J. Clemett⁴, D. Trang⁵, L. P. Keller³, R. Christoffersen⁴, and D. G. Agresti⁶. ¹Department of Earth, Atmospheric, and Planetary Sciences, Purdue University, West Lafayette, IN 47907, mthompson@purdue.edu, ²Department of Physics and Astronomy, Northern Arizona University, Flagstaff, AZ 86011, ³ARES, NASA Johnson Space Center, Houston, TX 77058, ⁴Jacobs, NASA Johnson Space Center, Houston, TX 77058, ⁵Hawai'i Institute of Geophysics and Planetology, University of Hawai'i at Mānoa, Honolulu, HI 96822, ⁶University of Alabama at Birmingham, Department of Physics, Birmingham, AL 35294.

Introduction: The surfaces of airless bodies experience solar wind irradiation and micrometeorite impacts, a process collectively known as space weathering [1]. These mechanisms alter the chemical composition, microstructure, and optical properties of surface materials and considerable work has been done to understand this phenomenon in lunar and ordinary chondritic materials, e.g., [2,3]. However, ongoing sample return missions Hayabusa2 to asteroid Ryugu and OSIRIS-REx to asteroid Bennu have prompted the need to study the effects of space weathering on hydrated, organic-rich materials, especially in the context of early results e.g., [4]. Understanding space weathering of these samples is critical for properly interpreting remote sensing data during asteroid encounters, for sample site selection, and for the eventual study of returned samples.

We can better understand space weathering of carbonaceous materials by simulating these processes in the laboratory, e.g., [5,6]. Recent experiments have shown that the changes in spectral characteristics of carbonaceous chondrites are not consistent among experiments, suggesting additional work is needed before these results can inform our understanding of spectral variations on asteroidal surfaces. Similarly, substantial work remains to characterize the chemical and microstructural effects of these processes in order to correlate these features with spectral changes. Here, we build on our previous work, presenting new results of the pulsed laser irradiation of the Murchison (CM2) meteorite to simulate micrometeorite impacts and the progressive space weathering of carbonaceous surfaces.

Samples and Methods: We rastered an Nd-YAG pulsed laser ($\lambda=1064$ nm, ~ 6 ns pulse duration, energy 48 mJ/pulse) 1x, 3x, and 5x over the surface of three individual, dry-cut rock chips of the Murchison meteorite. We collected reflectance spectra for the unirradiated and irradiated regions of the samples using an ASD FieldSpec 3 Spectrometer over the wavelength range of 0.35–2.5 μm . We analyzed the organic functional group chemistry at two photoionization wavelengths (266 nm for aromatics and 118 nm for overall organics) for the irradiated and unirradiated regions of the 1x and 5x lasered samples using the $\mu\text{L}^2\text{MS}$ instrument. Finally, we prepared electron-transparent thin sections using the FEI Quanta 3D focused ion beam (FIB) for analysis in

the JEOL 2500 transmission electron microscope (TEM) at JSC. We characterized the chemical and microstructural features of irradiated olivine and sulfide grains, as well as matrix material for each sample. Finally, we used a radiative transfer model to investigate the effects of sub-microscopic particles of varying compositions on the optical properties of silicate grains to improve interpretation of our data.

Spectral Analyses: The irradiated regions are all darker than the unirradiated material, but show progressive brightening with each laser raster, with the 5x lasered sample being 20% brighter than the 1x lasered sample. The slope of the reflectance spectra for the lasered surfaces range from 20–30% bluer than the unirradiated surface, although the degree of bluing decreases with increasing laser irradiation. We observe an initial strengthening and subsequent weakening of the 1.93 μm water feature, and a progressive weakening of other absorptions bands, including the 0.7 μm feature associated with phyllosilicates, further described in [7].

Organic Analyses: $\mu\text{L}^2\text{MS}$ spectral maps spanning the raw and irradiated regions of the 1x lasered sample show an increased abundance of simple free organics and in aromatic/conjugated organic material [7]. Similar analyses of the 5x lasered sample show a similar distribution of types of organic species between the irradiated and unirradiated regions of the sample but with a net increase in the concentration of aromatic species (Fig. 1).

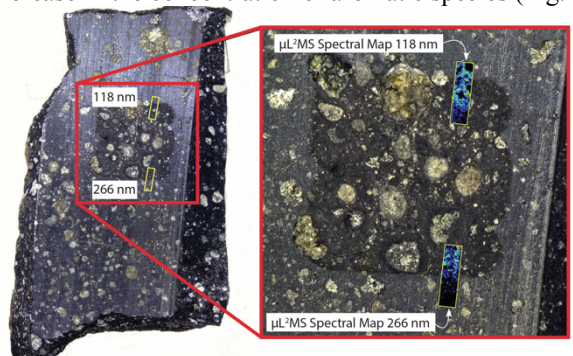


Figure 1: Organic analyses for the 5x lasered sample showing A) the $\mu\text{L}^2\text{MS}$ maps of the lasered and unlasered regions of the sample. The color bar represents organic concentration from low (blue) to high (red).

TEM Analysis: Results from the TEM reveal complex microstructural and chemical features.

Olivine: There are two amorphous, chemically distinct layers on the surface of the 5x lasered olivine. Energy dispersive x-ray spectroscopy (EDS) chemical maps indicate that the innermost layer (90 nm thick) has a composition consistent with the underlying olivine, suggesting a melt origin, and has Fe nanoparticles (<5 nm in size) uniformly distributed across the base. Superimposed on this layer is a 10 nm thick deposit which includes Fe, Ni and S in its composition, suggesting it is a vapor deposit sourced from elsewhere. High resolution TEM (HRTEM) images indicate the olivine maintains crystallinity up to the interface with the melt layer.

Sulfide: The 5x lasered sulfide shows a 10 nm thick deposit on the surface composed of Fe, O, and Si, suggesting it is a vapor deposit. HRTEM images indicate the deposit is amorphous and the underlying sulfide grain exhibits localized regions of amorphization intermixed with areas of nanocrystallinity.

Matrix: There is a surface melt layer, increasing in thickness from 500 nm to nearly 1 μm in the 1x and 5x lasered samples, respectively. The melt layer contains abundant nanoparticles, typically <10 nm in size in the 1x lasered sample and increasing in size up to 100 nm in the 5x lasered sample. HRTEM data and EDS maps of these deposits indicate the nanoparticles are Fe, Fe-Oxide (magnetite), Fe-S (troilite), and Fe-Ni-sulfides (pentlandite). The nanoparticles are dominated by Fe-Ni-sulfides in the 5x lasered sample (Fig. 2). HRTEM images indicate the degree of amorphization of matrix phases, in particular the phyllosilicates, increases with increasing laser irradiation.

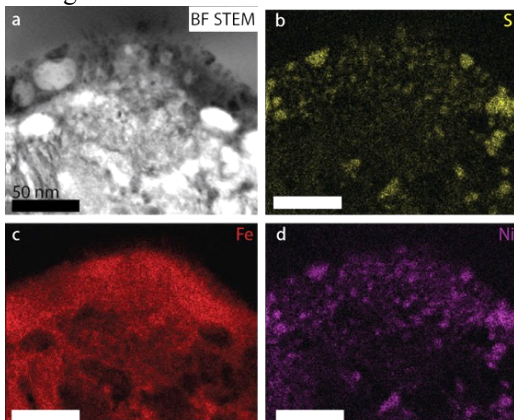


Figure 2: TEM data of the 5x lasered matrix. A) BF STEM, and EDS maps of B) S, C) Fe, and D) Ni.

Spectral Modeling: Nanophase (<40 nm) magnetite grains on the optical properties of quartz hosts cause an overall darkening of the spectrum which becomes more pronounced for microphase (>40 nm) particles. Both nano- and micro-phase magnetite nanoparticles cause bluing of the reflectance spectrum. In a similar model, but with inclusions troilite, both nano- and micro-phase particles show darkening. However, nano-

phase troilite causes strong reddening of the spectrum, whereas microphase particles cause bluing (Fig. 3).

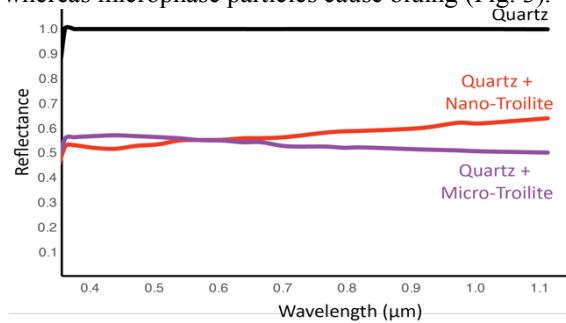


Figure 3: Spectral models showing the absolute reflectance of quartz (black), quartz with <40 nm inclusions of troilite (FeS) (red) and >40 nm inclusions (purple).

Implications for Primitive Asteroids: The results presented here provide further evidence that the space weathering of carbonaceous surfaces is a complex process, highlighting the importance of coordinated analyses to provide an improved understanding. As irradiation proceeds, the progressive brightening of samples relative to the dark state produced by the laser initially may be caused by increased surface roughness from the laser production of melt and vapor deposits. However, an additional brightening contribution might also come from increasing content of laser-altered organics on the surface as shown by the $\mu\text{L}^2\text{MS}$ measurements. This is suggested by the analogous observation of brightening in ion-processed carbonaceous chondrite organics [8].

The reflectance spectra of the irradiated regions also show bluing compared to the raw surface, the degree of which weakens with progressive lasering. To understand these spectral results we can look to our microstructural and chemical analyses and our spectral models. TEM analyses indicate that the nanoparticles are initially small and include diverse phases such as magnetite. With successive laser irradiation, the nanoparticles become larger and are compositionally dominated by Fe-Ni-sulfides. Our modelling results indicate that there are competing spectral effects (reddening vs. bluing) depending on the composition and size of the nanoparticles, with smaller Fe-Ni-sulfides causing reddening and larger nanoparticles bluing. The continued production of Fe-Ni-S particles may explain the weakening of the degree of bluing with successive irradiation.

References: [1] Pieters C.M. and Noble S.K. (2016) *J. Geophys. Res-Planet.*, 121, 1865-1884. [2] Keller L.P. and McKay D.S. (1993) *Science*, 261, 1305-1307. [3] Noguchi T. et al. (2011) *Science*, 333, 1121-1125. [4] Matsuoka M. et al. (2018) *Hayabusa Symposium*. [5] Matsuoka M. et al. (2015) *Icarus*, 254, 135-143. [6] Gillis-Davis J.J. et al. (2017) *Icarus*, 286, 1-14. [7] Thompson M.S. (2018) *LPS XXXIX Abstract #2083* [8] Moroz L. et al. (2004) *Icarus*, 170, 214-228.